Kinetics and Mechanism of Intercellular Ice Propagation in a Micropatterned Tissue Construct

Daniel Irimia* and Jens O. M. Karlsson*†
*Department of Bioengineering and †Department of Mechanical Engineering, University of Illinois, Chicago, Illinois 60607 USA

ABSTRACT Understanding the effects of cell–cell interaction on intracellular ice formation (IIF) is required to design optimized protocols for cryopreservation of tissue. To determine the effects of cell–cell interactions during tissue freezing, without confounding effects from uncontrolled factors (such as time in culture, cell geometry, and cell–substrate interactions), HepG2 cells were cultured in pairs on glass coverslips micropatterned with polyethylene glycol disilane, such that each cell interacted with exactly one adjacent cell. Assuming the cell pair to be a finite state system, being either in an unfrozen state (no ice in either cell), a singlet state (IIF in one cell only), or a doublet state (IIF in both cells), the kinetics of state transitions were theoretically modeled and cryomicroscopically measured. The rate of intercellular ice propagation, estimated from the measured singlet state probability, increased in the first 24 h of culture and remained steady thereafter. In cell pairs cultured for 24 h and treated with the gap junction blocker 18β-glycyrrhetinic acid before freezing, the intercellular ice propagation rate was lower than in untreated controls ($p < 0.001$), but significantly greater than zero ($p < 0.0001$). These results suggest that gap junctions mediate some, but not all, mechanisms of ice propagation in tissue.

INTRODUCTION

The improved understanding, in recent years, of many important biophysical processes taking place during cryopreservation of cell suspensions has led to the development of successful methods for cryopreservation of cells isolated from different tissues (McGrath, 1985) and the emerging use of theoretical models for rational design and optimization of cell cryopreservation protocols (Karlsson et al., 1996). In contrast, protocols for the preservation of native and engineered tissues by freezing to cryogenic temperatures are still far from satisfactory, because of the complexity of the systems and our limited understanding of the underlying biophysical processes (Karlsson and Toner, 1996). Our knowledge of the cryobiology of isolated cells cannot simply be extrapolated to tissues, inasmuch as the low temperature behavior of cells in tissue culture is quantitatively different from that of cells in suspension, and because additional biophysical phenomena (e.g., cell–cell and cell–substrate interactions, geometrical effects, heat and mass transport limitations in macroscopic systems) must be considered (Karlsson and Toner, 1996, 2000).

The probability of intracellular ice formation (IIF), a deleterious event during cryopreservation, is known to be enhanced in confluent monolayer cultures, as compared with either suspended or adherent isolated cells (Porsche et al., 1991; Yarmush et al., 1992; Larese et al., 1992; Armitage and Juss, 1996; Acker et al., 1999; Acker and McGann, 2000). Furthermore, the probability of IIF also appears to be enhanced in suspended cell clusters, as compared with suspensions of isolated cells (McGann et al., 1972, 1993; McGrath et al., 1975; Larese et al., 1992; Acker et al., 1999). Although such observations are suggestive of a role for cell–cell interactions in mediating IIF in tissue, these studies have introduced a host of confounding factors by comparing freshly trypsinized cells with cells cultured for various lengths of time in different configurations. To whit, the probability of IIF is known to be affected both by trypsinization (Sandler and Andersson, 1984; Yarmush et al., 1992) and time in culture (Hetzel et al., 1973; Hornung et al., 1996; Darr and Hubel, 2001); in cell clusters, mass transport limitations may also affect IIF (Levin et al., 1977).

The involvement of gap junctions in cell–cell interactions during freezing was first proposed by Berger and Uhrik, based on qualitative observations of the effect of gap junction inhibitors on IIF in cell strands from salivary gland tissue (Berger and Uhrik, 1992, 1996). A subsequent study provided indirect support for gap junction involvement in intercellular ice propagation, by comparing the kinetics of IIF in monolayers of two different cell lines, one of which (Madin-Darby canine kidney, MDCK) expresses gap junctions, and the other of which (V-79W fibroblasts) is believed not to express gap junctions (Yang et al., 1996). Recently, Acker et al. (2001) have followed up this initial report by correlating the effect of temperature on IIF in MDCK and V-79W monolayers with theoretical predictions of ice growth in pores (Mazur, 1960), and by studying the effect of low-calcium media (which disrupt intercellular junctions) on the pattern of IIF in MDCK cultures, adding further support to the gap junction hypothesis. In the present work, we report on intercellular ice propagation in HepG2 cells, a human hepatoma cell line that expresses connexin 32 and forms gap junctions (Jansen and Jongen, 1996; Yano et al., 2001).

The objective of the present study was to unambiguously quantify the effect of cell–cell interaction on IIF in tissue, and to investigate the role of gap junctions in intercellular ice

Submitted September 17, 2001, and accepted for publication November 8, 2001.

Address reprint requests to Jens O. M. Karlsson E-mail: karlsson@alum.mit.edu.

0006-3495/02/04/1858/11 $2.00

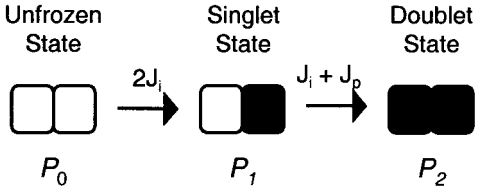

FIGURE 1 Schematic illustrating the IIF states of a cell pair, and the possible state transitions. Open blocks indicate unfrozen cells, whereas filled blocks indicate cells with internal ice. State transitions were modeled as sequential first-order reactions, with rate constants as shown. The state of an ensemble of cell pairs was described by the probabilities P_0, P_1, and P_2 of the unfrozen, singlet, and doublet state, respectively.

propagation. By using micropatterning techniques to control the attachment of cells onto a substrate, we have been able to create microscale tissue constructs consisting of a small number of cells in a reproducible configuration; such systems are attractive because their dynamics are sufficiently simple that they can be rigorously analyzed using theoretical mathematical models, thus permitting systematic testing of hypotheses about the mechanisms of IIF during tissue freezing. Moreover, unlike other experimental systems, our micropatterned tissue constructs make possible independent control of the degree of cell–cell contact, time in culture, tissue morphology, and other potentially confounding factors. In this work, we have used experiments and theoretical analysis to explore the hypothesis that IIF in tissue is governed by two stochastic processes: an independent IIF process not affected by the state of neighboring cells, and an intercellular ice propagation process, which is active only if ice is present in an adjoining cell. The contribution of these two processes to the probability of IIF was quantified in an engineered tissue construct consisting of two adjoining HepG2 cells micropatterned on a glass substrate. The effect of time in culture on the degree of cell–cell interaction was determined, and the involvement of gap junctions was investigated by studying the effects of a specific gap-junction blocker on the kinetics of intercellular ice propagation.

THEORETICAL BACKGROUND

To analyze our experimental results, we developed a theoretical model of the kinetics of IIF in an ensemble of cell pairs. As illustrated in Fig. 1, a pair of adjoining cells can assume only one of three IIF states: an unfrozen state (i.e., no ice in either cell), a partially frozen singlet state (i.e., ice present in only one of the cells), or a fully frozen doublet state (i.e., ice present in both cells). At any instant, in an ensemble of N cell pairs (i.e., $2N$ cells), there will be N_0 unfrozen pairs, N_1 partially frozen pairs, and N_2 fully frozen pairs, where $N_0 + N_1 + N_2 = N$. Thus, the state of the ensemble can be fully described by two state variables: the probability of the unfrozen state,

$$P_0 \equiv \frac{N_0}{N}, \tag{1}$$

and the probability of the singlet state

$$P_1 \equiv \frac{N_1}{N}. \tag{2}$$

The probability of the doublet state, defined

$$P_2 \equiv \frac{N_2}{N}, \tag{3}$$

is not an independent state variable, because

$$P_2 = 1 - P_0 - P_1. \tag{4}$$

We have assumed that the mechanisms of IIF in this system can be described by two stochastic processes, which we will call "independent ice formation" and "intercellular ice propagation," respectively. Independent ice formation is assumed to comprise all mechanisms for which the rate of IIF in a cell is independent of the state of the adjoining cell. Conversely, the intercellular ice propagation process describes the class of all mechanisms that can cause IIF in a cell if and only if ice is present in the adjoining cell. Thus, independent ice formation may be due to homogeneous, surface-catalyzed, or volume-catalyzed nucleation (Toner et al., 1990), to osmotic rupture (Muldrew and McGann, 1994), or other mechanisms. Likewise, intercellular ice propagation may be due to ice growth through gap junctions (Berger and Uhrik, 1996), or to surface-catalyzed nucleation mediated by intracellular ice in an adjoining cell. Because the probability of simultaneous IIF in both cells of a pair can be assumed to be infinitesimally small, the transition between IIF states can be described by a sequential reaction as shown in Fig. 1. Whereas the transition from the unfrozen to the singlet state is only possible via the independent ice formation process as defined above, the rate of consumption of unfrozen cell pairs (which equals the rate of singlet formation) is given by

$$\frac{dN_0}{dt} = -2J_iN_0, \tag{5}$$

where J_i is the average rate of independent ice formation events per unfrozen cell, and t is time. The singlet-to-doublet transition may occur either by the independent ice formation process or by intercellular ice propagation, so the rate of doublet formation (which equals the rate of singlet consumption) is given by

$$\frac{dN_2}{dt} = (J_i + J_p) \cdot N_1, \tag{6}$$

where J_p is the average rate of intercellular ice propagation events per unfrozen cell, given that ice is present in the adjoining cell.

To nondimensionalize the governing equations, we define a dimensionless time,

$$\tau \equiv \int_0^t J_i \, dt. \tag{7}$$

Furthermore, we define a dimensionless ice propagation rate,

$$\alpha \equiv \frac{J_p}{J_i}. \tag{8}$$

The dimensionless ice propagation rate α quantifies the degree of interaction between adjoining cells, and can therefore be interpreted as an interaction parameter in our system. Combining Eqs. 1–8, the kinetics of IIF in an ensemble of cell pairs can be described by the state equation,

$$\frac{d}{d\tau}\begin{bmatrix} P_0 \\ P_1 \end{bmatrix} = \begin{bmatrix} -2 & 0 \\ 2 & -(1+\alpha) \end{bmatrix} \cdot \begin{bmatrix} P_0 \\ P_1 \end{bmatrix}, \tag{9}$$

and the overall probability of IIF in the cell population is given by

$$P_{IIF} = 1 - P_0 - \tfrac{1}{2} P_1. \tag{10}$$

Noting that the kinetics of the unfrozen state (P_0) are decoupled from the kinetics of the singlet state (P_1), one obtains by inspection,

$$P_0(\tau) = e^{-2\tau}. \tag{11}$$

Whereas the interaction parameter α is typically a nonlinear function of time, there is no general analytical solution for $P_1(\tau)$.

It is illustrative, however, to consider the limiting case of no cell–cell interaction ($\alpha = 0$). In this case, the solution of Eq. 9 yields

$$P_1(\tau) = 2e^{-\tau} - 2e^{-2\tau}. \tag{12}$$

Considering that Eq. 11 can be inverted to solve for τ,

$$\tau = -\tfrac{1}{2} \cdot \ln P_0, \tag{13}$$

one obtains, by substituting Eq. 13 into Eq. 12,

$$P_1 = 2 \cdot (P_0^{1/2} - P_0). \tag{14}$$

Similarly, the overall probability of IIF when $\alpha = 0$ is given by

$$P_{IIF}(\tau) = 1 - e^{-\tau}, \tag{15}$$

which can be rewritten,

$$P_{IIF} = 1 - P_0^{1/2}. \tag{16}$$

Thus, even if there is intercellular ice propagation in the system ($\alpha > 0$), the observed kinetics of the unfrozen state can be used in conjunction with Eq. 16 to determine the hypothetical probability of intracellular ice formation due only to the independent ice formation process (J_i).

In the limiting case of instantaneous ice propagation ($\alpha \to \infty$), the probability of the singlet state vanishes, and

$$P_{IIF}(\tau) = 1 - e^{-2\tau}, \tag{17}$$

i.e., the overall rate of IIF is double the rate observed in the case of no propagation.

Eq. 9 can be solved analytically if the interaction parameter α is constant. Thus, one obtains

$$P_1(\tau) = \frac{2}{1-\alpha} \cdot (e^{-(1+\alpha)\cdot\tau} - e^{-2\tau}) \quad \text{for} \quad \alpha \neq 1, \tag{18}$$

$$P_1(\tau) = 2\tau \cdot e^{-2\tau} \quad \text{for} \quad \alpha = 1. \tag{19}$$

It can be shown that Eq. 18 reaches a maximum value,

$$P_1^* = \left(\frac{1+\alpha}{2}\right)^{(1+\alpha)/(1-\alpha)} \tag{20}$$

at

$$\tau^* = \frac{1}{1-\alpha} \cdot \ln\left[\frac{2}{1+\alpha}\right]. \tag{21}$$

MATERIALS AND METHODS

Preparation of micropatterned surfaces

Cell attachment and spreading can be controlled using polyethylene glycol (PEG), a biocompatible polymer that inhibits cell adhesion. We developed a micropatterning technique using a silanated form of PEG (Jo and Park, 2000), which enables surface modification of glass substrates in a single step, in contrast to conventional methods (Harris, 1992).

Glass coverslips (45 × 50 × 0.1 mm; Fisher Scientific, Pittsburgh, PA) were thoroughly cleaned with Sparkleen 1 detergent (Fisher) for 10 min and then rinsed with purified water (Elix 3 water purification system, Millipore, Bedford, MA) for 3 min. The remaining processing steps were carried out in a Class 100 clean room. The glass surfaces were cleaned again by immersion in Summa Clean SC15M solution (Mallinckrodt Baker, Paris, KY) in an ultrasound bath at 25°C for 10 min followed by a 10-min immersion in Piranha solution (25% v/v H_2SO_4, 75% v/v H_2O_2, Ashland Chemical, Columbus, OH). After a rinse in distilled water for 5 min, the coverslips were dried for 10 min at 90°C. Control coverslips to be used for unpatterned monolayer cultures were cleaned using the same method.

The coverslips were micropatterned using photolithographic techniques, as shown in Fig. 2. A thin layer (~1 μm) of positive photoresist 1818 (Shipley, Marlborough, MA) was applied by spin-coating at 5000 rpm for 30 s. The coverslips were then baked for 10 min at 90°C, and exposed for 10 s to 20 mW/cm^2 ultraviolet light in a mask aligner (Karl Suss, Waterbury Center, VT), using a chromium-glass mask with a pattern consisting of rectangular features of dimensions 30 × 80 μm and 30 × 40 μm separated by ~80 μm. The photoresist was then developed for 15 s using photoresist developer 351 (Shipley) followed by a 3-min rinse in distilled water, leaving islands of photoresist on a bare glass surface (Fig. 2 *A*); the resulting patterned features were checked by optical microscopy.

The coverslips were dehydrated at 90°C for 10 min, after which an aqueous solution of 5 mM PEG-disilane (Shearwater Polymers, Huntsville, AL) was applied (Fig. 2 *B*). After drying the coverslips at 75°C for 5 min,

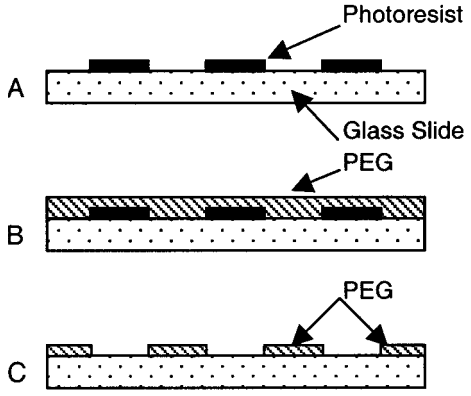

FIGURE 2 Preparation of micropatterned surfaces. (*A*) Photoresist was exposed to ultraviolet light through a patterned mask and developed, leaving islands of photoresist on the glass substrate. (*B*) The coverslip was then covered with a layer of PEG. (*C*) After photoresist removal, islands of bare glass surrounded by PEG were obtained.

the unexposed photoresist was removed by immersing the coverslips in photoresist remover UN2491 (Shipley) for 15 s (this time had been optimized to minimize adverse effects on the PEG layer), followed by a 5-min rinse in distilled water, leaving rectangular regions of bare glass surrounded by a thin layer of PEG (Fig. 2 *C*). Finally, the patterned coverslips were cut into 5 × 10-mm pieces with a diamond glass cutter.

Cell culture

The human hepatoma cell line HepG2 (American Type Culture Collection, Manassas, VA) was cultured at 37°C under a humidified 5% CO_2 atmosphere, in minimum essential medium (Gibco BRL Life Technologies, Rockville, MD) supplemented with 10% v/v bovine calf serum (Sigma-Aldrich, St. Louis, MO), 2.2 g/l sodium bicarbonate (Sigma), 1 mM sodium pyruvate (Sigma), 100 μg/ml streptomycin (Boehringer Mannheim, Indianapolis, IN) and 100 U/ml penicillin (Boehringer Mannheim). Media were replaced every two days and cell cultures were subcultivated once a week by disaggregation in a solution of 0.2% w/v trypsin (Gibco), 0.2% w/v glucose (Sigma), and 0.5 mM EDTA (Sigma) in isotonic Ca^{2+} and Mg^{2+} free Dulbecco's Phosphate Buffered Solution (PBS; Gibco), followed by resuspension in culture medium and replating at a subcultivation ratio of 1:5.

For experiments, HepG2 cells were trypsinized, suspended in culture media, and washed by centrifugation for 2.5 min at 200 × *g*, followed by aspiration of the supernatant media, resuspension in versene solution (5 mM EDTA in Ca^{2+} and Mg^{2+} free PBS), a second centrifugation (2.5 min at 200 × *g*), and aspiration of the supernatant versene. The cell pellet was resuspended in isotonic Ca^{2+} and Mg^{2+} free PBS, and either used directly in cryomicroscopy experiments (at a cell density of $\sim 1 \times 10^4$/ml), or cultured on glass coverslips in one- or two-cell patterns, or in confluent monolayers, as described below.

For cell micropatterning, the cell density was adjusted to 1×10^4/ml (for one-cell patterns) or 1×10^5/ml (for two-cell patterns), and 2 ml cell suspension was seeded onto patterned glass coverslips in a petri dish. The cells were incubated for 20 min at 37°C to allow cells to adhere to the exposed regions of the glass surface. Nonadherent cells were removed by flushing the coverslip with 5 ml culture media while simultaneously aspirating the supernatant, until 1–2 ml media were left in the culture dish. This procedure was necessary to prevent drying of the coverslip (due to the nonwetting properties of the patterned surfaces) and consequent cell damage. The petri dishes were immediately transferred to the incubator and cultured for either 12, 24, 36, or 48 h before use in experiments.

To create unpatterned monolayer cultures, the cell density was adjusted to 2×10^5/ml, such that the monolayer would be confluent after 24 hours. Cells were seeded onto unpatterned glass coverslips in petri dishes, followed by a 20-min incubation at 37°C and a media change, as described above for preparation of micropatterned cultures. Cells were cultured for 24 h before use in experiments.

Sample preparation

For experiments with adherent cells, the nucleic acid stain SYTO13 (Molecular Probes, Eugene, OR) was used to identify individual cells in a culture. SYTO13 has previously been shown not to influence the intracellular ice formation process (Acker and McGann, 2000). To investigate the role of gap junctions in intercellular ice propagation, 18β-glycyrrhetinic acid (GA; Sigma), a known gap-junction blocker (Davidson et al., 1986), was used. Coverslips were removed from the culture dishes and incubated for 10–15 min at 37°C in a solution of 2 μM SYTO13 in PBS with or without 30 μM GA. For cryomicroscopy experiments, a 2-μl droplet of this solution was transferred to an 18-mm-diameter circular glass coverslip (Fisher), onto which the cell culture coverslip was then inverted, forming a sandwich. For control experiments with suspended cells, a sandwich was formed by placing 7 μl of the cell suspension between two circular coverslips. All samples were used in experiments immediately after preparation.

Cryomicroscopy

IIF was observed during freezing of cultured and suspended cells using a cryomicroscopy system consisting of an upright Nikon Eclipse E600 research microscope fitted with a commercially available cooling stage (BCS 196; Linkam Scientific Instruments, Tadworth, Surrey, UK). The sample was cooled by heat conduction to a silver block in contact with a nitrogen gas stream, which was pre-cooled using a coiled copper tubing heat exchanger immersed in liquid nitrogen. The stage temperature was regulated using an electrical resistance heater and a platinum-resistance thermometer imbedded in the silver block, together with a CI93 feedback control system (Linkam) and the Linksys software (version 1.4; Linkam). The temperature-control system was calibrated by measuring the melting point of ice crystallized from a sample of purified water. Cell and tissue samples were observed using a 20× or 50× objective, and experiments were recorded using a DVC-0A analog video camera (Digital Video Camera Company, Austin, TX), and a Sony SVO-9500MD videocassette recorder. A VTO 232 video text overlay system (Linkam) was used to superimpose time and stage temperature data onto the video images.

Samples were prepared as described above, and placed on the silver block of the cryomicroscopy stage under a dry nitrogen atmosphere, to prevent water condensation. Ice formation was induced in the extracellular solution by cooling the sample from 37°C to −1.8°C, and touching the edge of the sample with the seeding block, a silver block integrated into the cooling stage and chilled to the temperature of the nitrogen coolant. The sample was held at −1.8°C until the growing extracellular ice was in contact with the cells in the field of view. A video image of the SYTO13-stained cell nuclei was acquired using epifluorescence, to identify the number and position of individual cells, after which brightfield illumination was resumed, and cooling of the sample was initiated. The stage was cooled to −60°C at a controlled rate of 130°C/min.

In cryomicroscopic observations, the formation of intracellular ice crystals is typically manifested as a sudden darkening of the cytoplasm, due to scattering of the transilluminating light. Thus, the temperature of IIF for each cell in the field of view could be determined by examining the video recording of the freezing experiment using frame-by-frame playback. The probability of IIF at any temperature was determined by dividing the number of darkened cells by the total number of observed cells. The probability of the unfrozen state (P_0) at any temperature was determined by

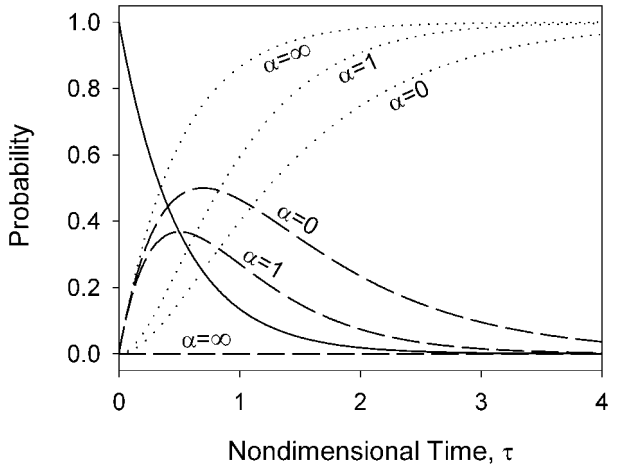

FIGURE 3 Theoretical prediction of the kinetics of IIF in an ensemble of cell pairs, for constant values of the dimensionless propagation rate, α. The probability of the unfrozen state, $P_0(\tau)$, (*solid line*) is independent of α, whereas the singlet state probability, $P_1(\tau)$, (*dashed lines*) and the doublet state probability, $P_2(\tau)$, (*dotted lines*) are shown for various values of α, as indicated.

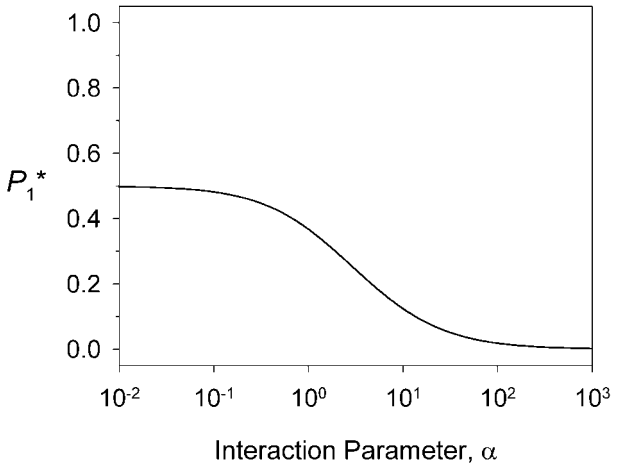

FIGURE 4 Theoretical prediction of the dependence of the maximum singlet state probability, P_1^*, on the dimensionless propagation rate (interaction parameter), α.

counting the number of cell pairs in which neither cell appeared dark, and dividing this number by the total number of cell pairs observed. The probability of the singlet state (P_1) at any temperature was determined by counting the number of cell pairs in which only one of the cells had darkened, and dividing this number by the total number of cell pairs observed. The probability of the doublet state (P_2) at any temperature was determined by counting the number of cell pairs in which both cells had darkened, and dividing this number by the total number of cell pairs observed. For each experimental condition, 60–280 cells were analyzed.

Statistical analysis

Data are reported as averages and standard errors of the mean. If groups had a normal distribution and homogenous variances, the group means were compared by an independent *t*-test, or by analysis of variance (ANOVA) followed by Fisher's least significant difference post-hoc test. A logarithmic transformation was applied to the data when group variances were not homogenous. The Kruskal–Wallis nonparametric test was used to compare populations that did not have a normal distribution. Differences were considered significant at the 95% confidence level ($p < 0.05$).

RESULTS

Predictions of the kinetics of IIF in an ensemble of cell pairs were obtained using Eqs. 4, 11, and 18, and are plotted for various values of the dimensionless ice propagation rate α in Fig. 3. The probability of the unfrozen state (P_0) decreases exponentially, and is independent of the rate of ice propagation. However, the rate of doublet formation increases with increasing α. The singlet state probability (P_1) exhibits a transient increase, because the singlet state is consumed upon formation of the doublet state. Thus, the higher the propagation rate α, the lower the probability of the singlet state. In particular, the maximum probability of the singlet state decreases with increasing α, as predicted by Eq. 20. As shown in Fig. 4, for values of α on the order of 0.1 to 100, the peak singlet state probability can be used as a measure of the magnitude of the dimensionless ice propagation rate.

To test the theoretical predictions of the effect of cell–cell interaction on the probability of IIF, HepG2 cells were cultured on glass coverslips for 24 h in micropatterned one-cell and two-cell configurations (shown in Fig. 5), or in confluent monolayers. Cultured cells and a control group of suspended cells were frozen to −60°C at a rate of 130°C/min. Figure 6 shows the resulting cumulative fraction of IIF (P_{IIF}), indicating a statistically significant effect of culture configuration on the mean IIF temperature ($p < 0.001$). In particular, suspended cells had the lowest probability of IIF (final $P_{IIF} = 81\%$), and the lowest mean temperature of IIF (-23.0 ± 1.1°C; sample size $n = 109$). For cultured cells, the final probability of IIF was 100% for all groups, and the mean IIF temperature increased with the number of cells

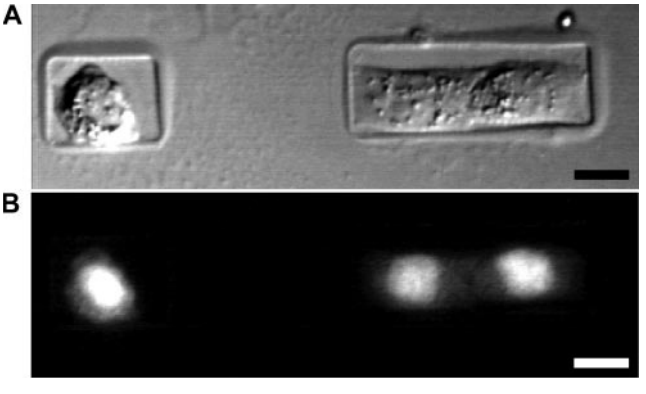

FIGURE 5 Micrograph of HepG2 cells cultured in one-cell (*left*) and two-cell (*right*) patterns. (*A*) Differential interference contrast. (*B*) Epifluorescence, with nuclear staining using SYTO13. Scale bars are 20 μm.

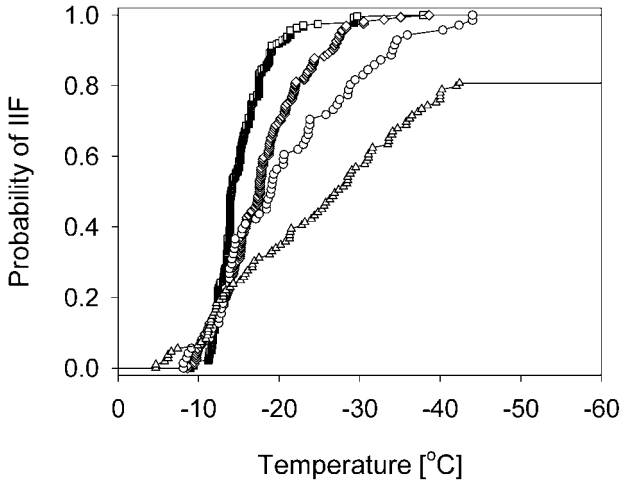

FIGURE 6 Cumulative probability of IIF in HepG2 cells cooled at 130°C/min to −60°C. Cells were either suspended in PBS (*triangles*) and immediately frozen, or cultured for 24 h on a glass substrate in one-cell patterns (*circles*), two-cell patterns (*diamonds*) or confluent monolayers (*squares*) before freezing.

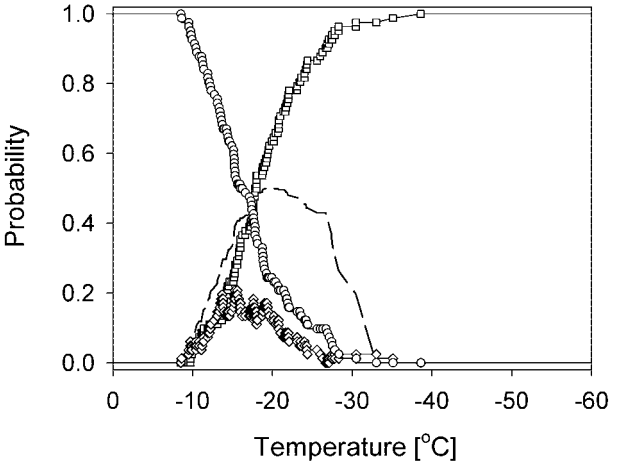

FIGURE 7 Probabilities of the unfrozen state, P_0, (*circles*) singlet state, P_1, (*diamonds*) and doublet state, P_2, (*squares*) during freezing of micropatterned cell pairs to −60°C at a rate of 130°C/min. Also shown is the hypothetical probability of the singlet state if there were no intercellular ice propagation ($\alpha = 0$) in this experiment, determined using Eq. 14 (*broken line*).

available for interaction. Thus, cells cultured in single-cell patterns had a mean IIF temperature of -21.0 ± 1.1°C ($n = 71$), cells cultured in pairs had a mean IIF temperature of -18.0 ± 0.4°C ($n = 164$), and cells cultured in confluent monolayers had a mean IIF temperature of -15.3 ± 0.2°C ($n = 278$). These observations were consistent with theoretical predictions of the effect of the interaction parameter α on P_{IIF}, as determined using Eqs. 10, 11, and 18 (results not shown).

Using the above cryomicroscopic observations of IIF during freezing of cells cultured in micropatterned pairs, the probabilities of the unfrozen (P_0), singlet (P_1), and doublet states (P_2) were determined as a function of temperature (Fig. 7). The observed kinetics are similar to the theoretical predictions shown in Fig. 3, with the number of unfrozen pairs decreasing monotonically, and the number of pairs in the singlet state exhibiting a transient increase. Using the measured probabilities of the unfrozen state together with Eq. 14, the probability of the singlet state for the hypothetical case of no intercellular ice propagation ($\alpha = 0$) was determined. As shown in Fig. 7, the actual singlet state probabilities were significantly lower than the corresponding probabilities for the hypothetical noninteracting case, indicating that intercellular ice propagation does occur during freezing of cultured HepG2 pairs. Furthermore, comparison of the observed singlet state probability peak ($P_1^* \sim 0.2$) with the results shown in Fig. 4, suggests that the dimensionless ice propagation rate is on the order of $\alpha \sim 5$.

Two sets of control experiments were designed to assess whether the rate of independent ice formation (J_i) was affected by the gap-junction blocker GA, by cell–cell contact, or by time in culture. Figure 8 shows the cumulative fraction of IIF (P_{IIF}) in cells cultured for 24 h in single-cell patterns, and frozen with or without a preceding GA treatment. Also shown in Fig. 8 are the results of freezing two-cell patterns with and without GA treatment. For the cell pairs, the measured probabilities of the unfrozen state (P_0) were transformed using Eq. 16 to determine the probability of IIF associated with the process of independent ice formation only. Comparison of the resulting IIF temperatures by two-way ANOVA revealed no significant effect of GA ($p > 0.4$), and no significant differences between one-cell and two-cell patterns ($p > 0.4$). Thus, the independent

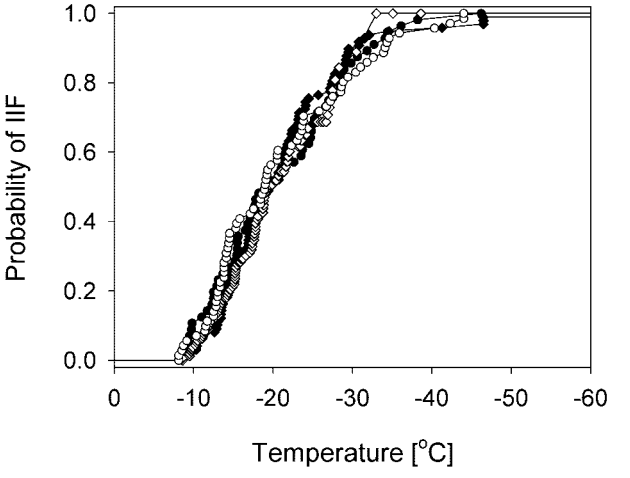

FIGURE 8 Kinetics of independent ice formation in cells cultured for 24 h in one-cell patterns (*circles*) and two-cell patterns (*diamonds*), with no pretreatment (*open symbols*) or pretreated with GA (*closed symbols*) prior to freezing at 130°C/min. For cell pairs, the probability shown is the hypothetical probability of IIF for independent ice formation only ($\alpha = 0$), determined using Eq. 16.

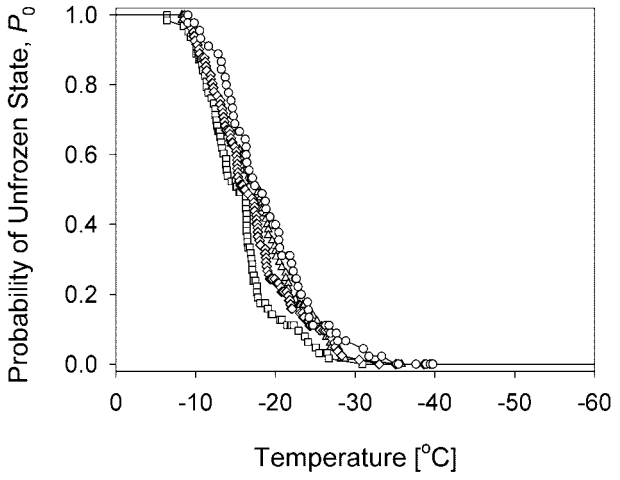

FIGURE 9 Probability of the unfrozen state (P_0) in micropatterned cell pairs cultured for 12 (*circles*), 24 (*diamonds*), 36 (*squares*), and 48 h (*triangles*) before freezing to −60°C at 130°C/min.

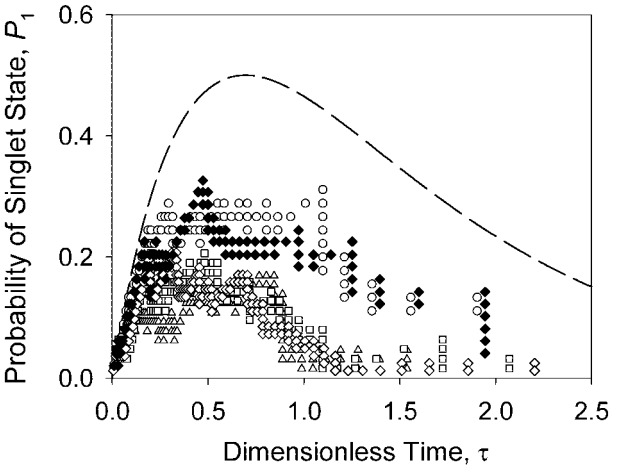

FIGURE 10 Effect of GA and time in culture on the probability of the singlet state (P_1) during cooling of cell pairs to −60°C at a rate of 130°C/min. Micropatterned pairs were either cultured for 24 h and treated with GA before freezing (*closed diamonds*), or cultured for 12 (*circles*), 24 (*open diamonds*), 36 (*squares*) or 48 hours (*triangles*) and frozen without GA treatment. Also shown are the theoretical predictions of $P_1(\tau)$ for the case of no cell–cell interaction ($\alpha = 0$), obtained using Eq. 12 (*broken line*).

ice formation process does not appear to be affected by cell–cell contact or by the presence of GA.

In the second control experiment, the effect of time in culture on the rate of independent ice formation was examined by comparing the kinetics of IIF in two-cell patterns frozen after 12, 24, 36, or 48 h in culture. Figure 9 shows the probability of the unfrozen state (P_0) for the four experimental groups, revealing no significant effect of time in culture on the mean temperature of singlet formation ($p > 0.05$). Whereas Eqs. 7 and 11 show that the kinetics of the unfrozen state do not depend on the intercellular ice propagation process, these results indicate that the rate of independent ice formation (J_i) in cell pairs is not affected by time in culture.

To examine the effect of GA and time in culture on intercellular ice propagation, the probabilities of the singlet state (P_1) were compared for cells cultured in a two-cell pattern for 12, 24, 36, or 48 h (without GA), and for two-cell constructs cultured for 24 h and treated with GA prior to freezing. By transformation of the measured probabilities of the unfrozen state (P_0) using Eq. 13, the measured singlet state probabilities could be plotted as a function of dimensionless time, and thus be directly compared to the analytical solution for noninteracting cells ($\alpha = 0$) obtained with Eq. 12. It is evident in Fig. 10 that the singlet state probabilities for all experimental groups were lower than the theoretical predictions of $P_1(\tau)$ for $\alpha = 0$, indicating that the rate of intercellular ice propagation was significant for all culture times, and for GA-treated cell pairs. Moreover, compared with cell pairs cultured for 24, 36, or 48 h in the absence of GA, there was a higher probability of the singlet state in cell pairs cultured for 12 h in the absence of GA, and in GA-treated cells, consistent with a lower rate of intercellular ice propagation in the latter groups.

Although the maximum singlet state probability is a measure of the interaction parameter α (see Fig. 4), estimating maximum values of P_1 from Fig. 10 would be problematic, due to the noise in the data. Thus, the time-averaged probability of the singlet state was used as an estimator for the rate of intercellular ice propagation. As shown in Fig. 11, the average singlet state probability was larger for cell pairs cultured for 12 h than that for cells cultured for 24 h ($p < 0.001$), indicating an increase in the rate of intercellular ice propagation with time in culture. There was a slight further decrease of the mean singlet state probability for culture times longer than 24 h, but this effect was not statistically significant ($p > 0.05$). For cell pairs cultured for 24 h, there was a significant effect of GA on the probability of the singlet state ($p < 0.001$), with a 64% increase in the average singlet state probability in the presence of the gap-junction blocker. The mean singlet state probability for the hypothetical case of no intercellular ice propagation ($\alpha = 0$) was 0.36 ± 0.01, as determined using data from cells cultured for 24 h without GA, transformed with Eq. 14. As shown in Fig. 11, the average singlet state probabilities for all experimental groups were significantly lower than that for the hypothetical noninteracting case ($p < 0.0001$), indicating that intercellular ice propagation was significant, even for cells treated with the gap-junction blocker.

The kinetics of the intercellular ice propagation process were analyzed by examining the singlet state persistence time Δt, i.e., the time difference between the two IIF events in each micropatterned cell pair. Figure 12 shows the cumulative probability distribution of Δt for two-cell constructs cultured for 12, 24, 36, or 48 h in the absence of GA,

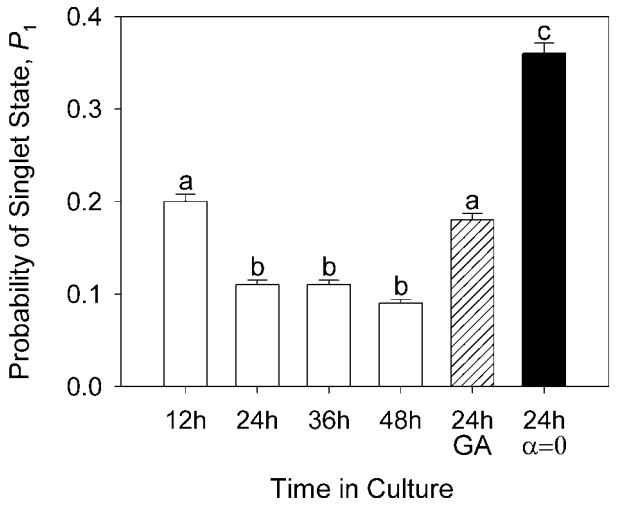

FIGURE 11 Mean values and standard errors of singlet state probabilities (P_1) from Fig. 10, showing the effect of GA and time in culture. Cell pairs were either cultured for 12–48 h and frozen (*white bars*), or cultured for 24 h and treated with GA before freezing (*hatched bar*). Also shown is the average singlet state probability for the hypothetical case of no intercellular ice propagation ($\alpha = 0$), determined using Eq. 14 (*black bar*). The singlet state probabilities are significantly different for bars with different superscript letters ($p < 0.001$).

and for cell pairs cultured for 24 h and treated with GA before freezing. Comparison of the probability distributions using a Kruskal–Wallis test revealed that the distributions for cells cultured for 24, 36, and 48 h in the absence of GA were statistically indistinguishable ($p > 0.7$), as were the distributions for cells cultured for 12 h and cells treated with GA ($p > 0.6$). For cell pairs cultured for 24 h, the distribution of singlet state persistence times for cells treated with GA was significantly different from the distribution for untreated cells ($p < 0.05$). Likewise, for cells not treated with GA, the distribution for cell pairs cultured for 12 h was significantly different from the distributions for longer culture times ($p < 0.05$).

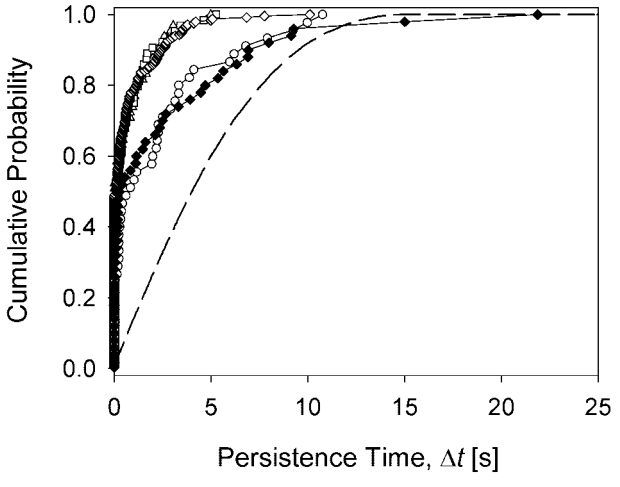

FIGURE 12 Cumulative probability distribution of singlet state persistence time, showing the effect of GA and time in culture. Micropatterned pairs were either cultured for 24 h and treated with GA before freezing (*closed diamonds*), or cultured for 12 (*circles*), 24 (*open diamonds*), 36 (*squares*), or 48 hours (*triangles*) and frozen without GA treatment. Also shown is the predicted distribution for the case of no cell–cell interaction ($\alpha = 0$), determined using Eq. 16 (*broken line*).

All observed singlet state persistence time distributions in Fig. 12 exhibited what appeared to be two subpopulations with distinct propagation kinetics. For each experimental group, about half of the propagation events occurred rapidly, within approximately 0.3 s of the initial IIF event. The lag times between successive IIF events in the remaining cell pairs were significantly longer, typically allowing the singlet state to persist for many seconds. The observed effects of GA and culture time appeared to have a much more marked effect on the distribution of slower propagation events than on the distribution of rapid propagation events. In fact, in cell pairs cultured for 12 h or treated with GA, the singlet subpopulation with $\Delta t > 0.3$ s had a persistence time distribution similar to that of noninteracting cell pairs (calculated from the probability of independent ice formation in cell pairs cultured for 24 h, using Eq. 16 and a random variable transformation).

DISCUSSION

Almost all previous investigations of the effect of cell–cell interactions on the IIF process have compared freshly trypsinized cells in suspension, or single cells adherent to glass, with cells of the same type cultured in confluent monolayers on glass (e.g., Porsche et al., 1991; Armitage and Juss, 1996; Acker and McGann, 2000), or suspension cultured in aggregates (e.g., McGann et al., 1972; McGrath et al., 1975; Acker et al., 1999). However, previous experimental designs have been unable to control confounding effects resulting from cell damage by enzymatic digestion (McGann et al., 1972; Sandler and Andersson, 1984; Yarmush et al., 1992), from changes in phenotype due to time in culture (Hetzel et al., 1973; Darr and Hubel, 2001) or cell attachment and spreading (Hornung et al., 1996; Chen et al., 1997), or from mass transport limitations in cell clusters (Levin et al., 1977). Whereas all aforementioned factors affect IIF and cryoinjury, past attempts to attribute differences in probability of IIF or cell survival for different culture configuration to hypothesized effects of cell–cell contact have not been conclusive.

Surface modification and micropatterning techniques have previously been used to control cell shape, position, and cell–cell contact in studies of the biological effects of cell adhesion and tissue coculture (Bhatia et al., 1997; Chen et al., 1997). In the present study, we have used similar techniques to probe the effect of cell–cell interactions on the IIF process, while eliminating confounding factors that have limited previous investigations of tissue freezing. In

particular, our experimental system is the first that permits independent control of cell–cell contact, cell shape, substrate interactions, and time in culture. Thus, by comparing the probability of IIF in micropatterned one- and two-cell constructs, which had been cultured for the same length of time on the same substrate, and in which each cell was constrained to occupy approximately the same surface area, the effect of cell–cell contact on IIF could be isolated. In micropatterned HepG2 cultures, the rate of IIF was observed to increase in the presence of cell–cell contact, and with time in culture.

Although increases in the probability of IIF in the presence of cell–cell contact have commonly been attributed to propagation of ice from one cell to neighboring cells, published evidence for such ice propagation has been mostly anecdotal in nature (Stuckey and Curtis, 1938; Brown and Reuter, 1974; Brown, 1980; Tsuruta et al., 1998; Acker et al., 1999). To the best of our knowledge, only three previous studies have attempted to quantify intercellular ice propagation. Berger and Uhrik (1996) counted the number of cell strands in which IIF occurred sequentially, finding that IIF was sequential in 10 out of 14 strands frozen. Acker and McGann (1998) defined a ratio of the number of cell–cell contacts in which both cells were frozen to the total number of frozen cells, finding that the value of this ratio was significantly larger than the value obtained from a Monte Carlo simulation of random IIF in a monolayer. In a subsequent study, Acker et al. (2001) evaluated the percentage of IIF events that occurred in cells not in contact with frozen cells, and observed that all IIF events observed in MDCK held at -3°C or below occurred in cells adjacent to previously frozen cells (Acker et al., 2001). In the present work, we have explicitly defined the rate of intercellular ice propagation as the increase in the rate of IIF associated with the formation of ice in an adjoining cell, and we have been able to quantify this rate by analyzing experimental data using a new theoretical model of ice propagation.

The ability to quantify the process of intercellular ice propagation is critical for understanding IIF in tissue, inasmuch as it is hypothetically possible that the observed effects of cell–cell contact, GA treatment, and time in culture on the probability of IIF in tissue constructs were due to nonpropagative mechanisms of IIF. For example, gene expression in HepG2 has been shown to be affected by cell–cell contact and time in culture (Kelly and Darlington, 1989). Whereas some nucleation-based mechanisms of IIF are thought to involve catalysis by intracellular proteins (Toner et al., 1990), it is possible that the increased probability of IIF in the presence of cell–cell contact and as a function of time in culture was due to expression of new heterogeneous nucleation sites. Similarly, other proposed mechanisms of IIF, such as osmotic or mechanical rupture, may be affected by changes in the cell's mechanical properties with time in culture (Ingber et al., 1994). Because most previous investigations have used only the overall probability of IIF or survival rate to assess the effect of tissue culture on IIF, it has hitherto not been possible to exclude such alternative hypotheses. However, our experiments have established that, if the substrate material and surface area for cell adhesion are controlled, the rate of independent ice formation (J_i) is not affected by cell–cell contact, time in culture, or GA treatment. Therefore, the observed effects of these factors on the probability of IIF were due only to changes in the rate of intercellular ice propagation (J_p).

Several mechanisms for intercellular ice propagation have been proposed in the literature, but none have been conclusively established. For example, McGann et al. (1972) speculated that cells ruptured by IIF released lysosymal enzymes that caused membrane damage, and hence IIF, in adjoining cells. Others have proposed that surface-catalyzed nucleation (Toner et al., 1990) in a supercooled cell may be mediated by ice crystals present in a neighboring cell (Tsuruta et al., 1998; Acker and McGann, 1998). Berger and Uhrik (1992, 1996) first suggested the involvement of intercellular channels in ice propagation, reporting that the sequence of IIF events in cell strands pretreated with the gap-junction blockers dinitrophenol or heptanol appeared to be random, whereas it was typically sequential in untreated strands. Recently, Acker et al. (2001) have used low-Ca^{2+} media to inhibit gap-junction formation in MDCK monolayers, and observed an increase in the number of independent IIF sites. Our present results lend support to the hypothesis that gap junctions are involved in intercellular ice propagation, but suggest that other mechanisms are also active.

We used the sapogenin 18β-glycyrrhetinic acid to block gap junctions, and found that the rate of intercellular ice propagation decreased in GA-treated cell pairs. Whereas low-Ca^{2+} media can disrupt tight junctions (Armitage et al., 1994) and anchoring junctions (Tozer et al., 1996) in addition to gap junctions, glycyrrhetinic acid inhibits gap junctions with high specificity (Davidson et al., 1986; Davidson and Baumgarten, 1988). Although the exact mechanism of action of GA is not fully known, it is not thought to be mediated by protein kinase C or steroid receptors (Davidson et al., 1986; Davidson and Baumgarten, 1988). For short exposure times, such as those used in the present study, GA does not appear to affect connexin phosphorylation or reduce the number of gap-junction plaques (Guan et al., 1996). Rather, it is thought that GA binds the gap-junction connexon, inducing a conformational change that closes the channel (Davidson and Baumgarten, 1988; Guan et al., 1996). Thus, our results suggest that intercellular ice propagation is mediated by active gap junctions, either by growth of ice crystals through the intercellular channels (Acker et al., 2001), or by the creation of a heterogeneous nucleation site on one side of the junction via conformational changes induced by intracellular ice on the other side of the junction.

Intercellular ice propagation was only partially inhibited by GA, suggesting that there are several mechanisms of ice propagation in tissue, some of which do not require the presence of open gap junctions. This hypothesis is sup-

ported by observations of ice propagation in V-79W fibroblasts, a cell line that has been claimed not to express gap junctions (Acker and McGann, 1998; Acker et al., 2001). Of course, the possibility exists that the V-79W strain does, like wild-type V-79, form some gap junctions (e.g., el-Fouly et al., 1987; Jongen et al., 1987). Likewise, it is possible that GA failed to completely block gap junctions in the present study. However, GA has been shown to completely inhibit fluorescent dye coupling in rat hepatocytes at concentrations of 10–20 μM after 15 min exposure (Lee and Rhee, 1998), and metabolic cooperation in fibroblasts with a median effective concentration 2 μM (Davidson and Baumgarten, 1998). In contrast, a 10% incidence of dye coupling was observed in an epithelial cell line after 15 min exposure to 40 μM GA (Guan et al., 1996). The 18α-glycyrrhetinic acid isoform of GA has been observed to completely inhibit dye coupling in hepatocytes at concentrations of 20–30 μM with exposure times of 5–10 min (Tordjmann et al., 1997; Eugenin et al., 1998). To account for the rate of intercellular ice propagation we observed following gap-junction inhibition, approximately 30% of the cell pairs would have to remain coupled after exposure to 30 μM GA for 15 min (Irimia and Karlsson, 2001). Thus, it seems likely that there exist mechanisms of ice propagation that do not require intercellular channels.

The distribution of singlet state persistence times (Fig. 12) was consistent with the hypothesis of two mechanisms of propagation, one fast ($\Delta t < 0.3$ s), and one slow ($0.3 \text{ s} < \Delta t < 5$ s). Decoupling cell–cell communication with GA appeared to have a more pronounced effect on the slower propagation mechanism (increasing the range of persistence times to $\Delta t <$ 20 s, comparable to the distribution of persistence times in noninteracting cells) than on the faster mechanism, suggesting that the former is associated with propagation via gap junctions. These results contrast somewhat with observations of IIF in coupled salivary gland cells, in which the average time delay between propagation events was in the range 0.2–0.3 s (Berger and Uhrik, 1996). However, inasmuch as freezing conditions and cell types were different in the present study, direct comparison of results is difficult.

Finally, our results indicate that, although the rate of independent IIF appears to be insensitive to time in culture for the time points tested, the rate of intercellular ice propagation increased with time in culture, reaching a steady-state value within approximately 24 h. Interestingly, the probability and kinetics of ice propagation in cell pairs cultured for 12 h were equivalent to results obtained upon inhibition of gap junctions with GA. We believe that, in our system, gap junctions did not reassemble following trypsinization until after 12 h, consistent with observations that gap junctions in trypsinized epithelial cells did not form until after 24–48 h in culture, remaining at a steady level of expression thereafter (Meller, 1979; Guo et al., 1999). The similarity in probability and kinetics of intercellular ice propagation following trypsinization and GA treatment suggests that, in both cases, gap junctions were completely blocked or disrupted, lending further support to the hypothesized existence of gap-junction independent mechanisms of ice propagation.

CONCLUSION

We have shown that cell–cell interactions increase the probability of IIF in tissue, and that this increase results not from nonspecific increases in the rate of IIF, but is due to the enabling of propagative ice formation processes upon cell–cell contact. At least one mechanism of intercellular ice propagation appears to depend on the presence of active gap junctions, as demonstrated by the reduction of the ice propagation rate following gap-junction blocking by GA. However, observations presented here and elsewhere also support the hypothesis that intercellular ice propagation can occur via mechanisms that do not involve gap junctions. Furthermore, our results suggest that gap-junction-independent ice propagation is faster than gap-junction-dependent ice propagation. Understanding the mechanisms of IIF during tissue cryopreservation is critical for predicting cryoinjury in multicellular systems. Thus, to extend previous successes in model-based rational design of cell-freezing protocols to emerging applications in tissue and organ preservation, further research must be done to fully elucidate the mechanisms of independent IIF and intercellular ice propagation in these complex system.

The authors gratefully acknowledge the helpful advice of Prof. Sangeeta N. Bhatia, who suggested the use of silanated PEG for surface modification. All microfabrication procedures were performed in the University of Illinois at Chicago Microfabrication Applications Laboratory. The work was funded by a National Science Foundation Faculty Early Career Development Award to J.O.M.K. (Grant No. BES-9875569).

REFERENCES

Acker, J. P., J. A. W. Elliot, and L. E. McGann. 2001. Intercellular ice propagation: experimental evidence for ice growth through membrane pores. *Biophys. J.* 81:1389–1397.

Acker, J. P., A. Larese, H. Yang, A. Petrenko, and L. E. McGann. 1999. Intracellular ice formation is affected by cell interactions. *Cryobiology.* 38:363–371.

Acker, J. P., and L. E. McGann. 1998. The role of cell–cell contact in intracellular ice formation. *Cryo Lett.* 19:367–374.

Acker, J. P., and L. E. McGann. 2000. Cell–cell contact affects membrane integrity after intracellular freezing. *Cryobiology.* 40:54–63.

Armitage, W. J., and B. K. Juss. 1996. The influence of cooling rate on survival of frozen cells differs in monolayers and suspensions. *Cryo Lett.* 17:213–218.

Armitage, W. J., B. K. Juss, and D. L. Easty. 1994. Response of epithelial (MDCK) cell junctions to calcium removal and osmotic stress is influenced by temperature. *Cryobiology.* 31:453–460.

Bhatia, S. N., M. L. Yarmush, and M. Toner. 1997. Controlling cell interactions by micropatterning in co-cultures: hepatocytes and 3T3 fibroblasts. *J. Biomed. Mater. Res.* 34:189–199.

Berger, W. K., and B. Uhrik. 1992. Dehydration and intracellular ice formation during freezing in single cells and in cell strands from salivary glands. *Cryobiology.* 29:715–716. (Abstr.)

Berger, W. K., and B. Uhrik. 1996. Freeze-induced shrinkage of individual cells and cell-to-cell propagation of intracellular ice in cell chains from salivary glands. *Experientia.* 52:843–850.

Brown, M. S. 1980. Freezing of nonwoody plant tissues. IV. Nucleation sites for freezing and refreezing of onion bulb epidermal cells. *Cryobiology.* 17:184–186.

Brown, M. S., and F. W. Reuter. 1974. Freezing of nonwoody plant tissues: III. Videotape micrography and the correlation between individual cellular freezing events and temperature changes in the surrounding tissue. *Cryobiology.* 11:185–191.

Chen, C. S., M. Mrksich, S. Huang, G. M. Whitesides, and D. E. Ingber. 1997. Geometric control of cell life and death. *Science.* 276:1425–1428.

Davidson, J. S., and I. M. Baumgarten. 1988. Glycyrrhetinic acid derivatives: a novel class of inhibitors of gap-junctional intercellular communication. Structure-activity relationships. *J. Pharmacol. Exp. Ther.* 246:1104–1107.

Davidson, J. S., I. M. Baumgarten, and E. H. Harley. 1986. Reversible inhibition of intercellular junctional communication by glycyrrhetinic acid. *Biochem. Biophys. Res. Commun.* 134:29–36.

Darr, T. B., and A. Hubel. 2001. Postthaw viability of precultured hepatocytes. *Cryobiology.* 42:11–20.

Eugenin, E. A., H. Gonzales, C. G. Saez, and J. C. Saez. 1998. Gap junctional communication coordinates vasopressin-induced glycogenolysis in rat hepatocytes. *Am. J. Physiol. Gastrointest. Liver Physiol.* 274:G1109–G1116.

el-Fouly, M. H., J. E. Trosko, and C. C. Chang. 1987. Scrape-loading and dye transfer. A rapid and simple technique to study gap junctional intercellular communication. *Exp. Cell Res.* 168:422–430.

Guan, X., S. Wilson, K. K. Schlender, and R. J. Ruch. 1996. Gap-junction disassembly and connexin 43 dephosphorylation induced by 18β-glycyrrhetinic acid. *Mol. Carcinog.* 16:157–164.

Guo, Y., C. Martinez-Williams, K. A. Gilbert, and D. E. Rannels. 1999. Inhibition of gap junction communication in alveolar epithelial cells by 18α-glycyrrhetinic acid. *Am. J. Physiol. Lung Cell Mol. Physiol.* 276: L1018–L1026.

Harris, J. M. 1992. Poly(Ethylene Glycol) Chemistry—Biotechnical and Biomedical Applications. Plenum Press, New York.

Hetzel, F. W., J. Kruuv, L. E. McGann, and H. E. Frey. 1973. Exposure of mammalian cells to physical damage: effect of the state of adhesion on colony-forming potential. *Cryobiology.* 10:206–211.

Hornung, J., T. Müller, and G. Fuhr. 1996. Cryopreservation of anchorage-dependent mammalian cells fixed to structured glass and silicon substrates. *Cryobiology.* 33:260–270.

Ingber, D. E., L. Dike, L. Hansen, S. Karp, H. Liley, A. Maniotis, H. McNamee, D. Mooney, G. Plopper, J. Sims, and W. Ning. 1994. Cellular tensegrity: exploring how mechanical changes in the cytoskeleton regulate cell growth, migration, and tissue pattern during morphogenesis. *Int. Rev. Cytol.* 150:173–224.

Irimia, D., and J. O. M. Karlsson. 2001. Cell–cell interaction during tissue freezing: quantitative investigation of intercellular ice propagation using a micropatterning technique. *Proc. Meeting Soc. Cryobiology, 38th,* Edinburgh. 83. (Abstr.)

Jo, S., and K. Park. 2000. Surface modification using silanated poly(ethylene glycol)s. *Biomaterials.* 21:605–616.

Jansen, L. A. M., and W. M. F. Jongen. 1996. The use of initiated cells as a test system for the detection of inhibitors of gap junctional intercellular communication. *Carcinogenesis.* 17:333–339.

Jongen, W. M., B. J. van der Leede, C. C. Chang, and J. E. Trosko. 1987. The transport of reactive intermediates in a co-cultivation system: the role of intercellular communication. *Carcinogenesis.* 8:1239–1243.

Karlsson, J. O. M., A. Eroglu, T. L. Toth, E. G. Cravalho, and M. Toner. 1996. Fertilization and development of mouse oocytes cryopreserved using a theoretically optimized protocol. *Hum. Reprod.* 11:1296–1305.

Karlsson, J. O. M., and M. Toner. 1996. Long-term storage of tissues by cryopreservation: critical issues. *Biomaterials.* 17:243–256.

Karlsson, J. O. M., and M. Toner. 2000. Cryopreservation. *In* Principles of Tissue Engineering. R. P. Lanza, R. Langer, and J. Vacanti, editors. Academic Press, San Diego, CA. 293–308.

Kelly, J. H., and G. J. Darlington. 1989. Modulation of the liver specific phenotype in the human hepatoblastoma line Hep G2. *In Vitro Cell. Dev. Biol.* 25:217–222.

Larese, A., H. Yang, A. Petrenko, and L. E. McGann. 1992. Intracellular ice formation is affected by cell to cell contact. *Cryobiology.* 29:728. (Abstr.)

Lee, M. J., and S. K. Rhee. 1998. Heteromeric gap junction channels in rat hepatocytes in which the expression of connexin26 is induced. *Mol. Cells.* 8:295–300.

Levin, R. L., E. G. Cravalho, and C. E. Huggins. 1977. Water transport in a cluster of closely packed erythrocytes at subzero temperatures. *Cryobiology.* 14:549–558.

Mazur, P. 1960. Physical factors implicated in the death of microorganisms at subzero temperatures. *Ann. NY Acad. Sci.* 85:610–629.

McGann, L. E., J. Kruuv, and H. E. Frey. 1972. Repair of freezing damage in mammalian cells. *Cryobiology.* 9:496–501.

McGann, L. E., H. Yang, Z. Huang, A. Petrenko, and A. Larese. 1993. Cell-to-cell and cell-to-surface interactions affect responses during cryopreservation. *Transfusion.* 33:611. (Abstr.)

McGrath, J. J. 1985. Preservation of biological material by freezing and thawing. *In* Heat Transfer in Medicine and Biology. Vol. 2. A. Shitzer and R. C. Eberhart, editors. Plenum Press, New York. 185–238.

McGrath, J. J., E. G. Cravalho, and C. E. Huggins. 1975. An experimental comparison of intracellular ice formation and freeze–thaw survival of HeLa S-3 cells. *Cryobiology.* 12:540–550.

Meller, K. 1979. The formation of gap and tight junctions between retinal pigment cells in cell cultures. *J. Neurocytol.* 8:229–238.

Muldrew, K., and L. E. McGann. 1994. The osmotic rupture hypothesis of intracellular freezing injury. *Biophys. J.* 66:532–541.

Porsche, A. M., C. Körber, and G. Rau. 1991. Freeze thaw behavior of cultured (bovine corneal) endothelial cells: suspension vs. monolayer. *Cryobiology.* 28:545. (Abstr.)

Sandler, S., and A. Andersson. 1984. The significance of culture for successful cryopreservation of isolated pancreatic islets of Langerhans. *Cryobiology.* 21:503–510.

Stuckey, I. H., and O. F. Curtis. 1938. Ice formation and the death of plant cells by freezing. *Plant Physiol.* 13:815–833.

Tordjmann, T., B. Berthon, M. Claret, and L. Combettes. 1997. Coordinated intercellular calcium waves induced by noradrenaline in rat hepatocytes: dual control by gap junction permeability and agonist. *EMBO J.* 16:5398–5407.

Toner, M., E. G. Cravalho, and M. Karel. 1990. Thermodynamics and kinetics of intracellular ice formation during freezing of biological cells. *J. Appl. Phys.* 67:1582–1593. Erratum: 1991. *J. Appl. Phys.* 10:4653.

Tozer, E. C., P. E. Hughes, and J. C. Loftus. 1996. Ligand binding and affinity modulation of integrins. *Biochem. Cell Biol.* 74:785–798.

Tsuruta, T., Y. Ishimoto, and T. Masuoka. 1998. Effects of glycerol on intracellular ice formation and dehydration of onion epidermis. *Ann. NY Acad. Sci.* 858:217–226.

Yang, H., X. M. Jia, S. Ebertz, and L. E. McGann. 1996. Cell junctions are targets for freezing injury. *Cryobiology.* 33:672–673. (Abstr.)

Yano, T., F. J. Hernandez-Blazquez, Y. Omori, and H. Yamasaki. 2001. Reduction of malignant phenotype of HEPG2 cell is associated with the expression of connexin 26 but not connexin 32. *Carcinogenesis.* 22: 1593–1600.

Yarmush, M. L., M. Toner, J. C. Y. Dunn, A. Rotem, A. Hubel, and R. G. Tompkins. 1992. Hepatic tissue engineering. Development of critical technologies. *Ann. NY Acad. Sci.* 665:238–252.